J Therm Anal Calorim (2010) 101:153–159
DOI 10.1007/s10973-009-0548-8

Thermal decomposition of silylated layered double hydroxides

Qi Tao · Hongping He · Ray L. Frost · Peng Yuan · Jianxi Zhu

Received: 2 June 2009 / Accepted: 7 October 2009 / Published online: 5 November 2009

Abstract Anionic surfactant and silane modified layered double hydroxides (LDHs) were synthesized through an in situ coprecipitation method. The structure and morphology were characterized by XRD and TEM techniques, and their thermal decomposition processes were investigated using infrared emission spectroscopy (IES) combined with thermogravimetry (TG). The surfactant modified LDHs (H-DS) shows three diffractions located at 1–7° (2θ), while there is only one broad reflection for silane grafted LDHs (H–Si) in this region. The morphologies of the H-DS and H–Si show fibrous exfoliated layers and curved sheets, respectively. The IES spectra and TG curves indicate that alkyl chain combustion and dehydroxylation are overlapped with each other during heating from 373 to 723 K in H-DS and to 873 K in H–Si. Sulfate anion transformation process occurs at 473 K in H-DS and 523 K in H–Si. The derivant of sulfate can exist even above 1073 K. After further decomposition, the metal oxides and the new type of Si–O compounds are formed beginning at around 923 K in silane modified sample.

Q. Tao · H. He · P. Yuan · J. Zhu
Guangzhou Institute of Geochemistry, Chinese Academy of Sciences, Guangzhou 510640, China

Q. Tao · H. He (✉) · R. L. Frost
Inorganic Materials Research Program, School of Physical and Chemical Sciences, Queensland University of Technology, GPO Box 2434, Brisbane, QLD 4001, Australia
e-mail: hehp@gig.ac.cn

R. L. Frost
e-mail: r.frost@qut.edu.au

Q. Tao
Graduate School of Chinese Academy of Sciences, Beijing 100039, China

Keywords Anionic surfactant · IES · Layered double hydroxides · Silylation · TG

Introduction

Layered double hydroxides (LDHs), also known as hydrotalcites (Ht), can be easily described as trivalent cations substituted brucite layers with the surface charges balanced by interlayer anions. They are commonly expressed as $[M_{1-x}^{2+}M_x^{3+}(OH)_2]^{x+}A_{x/n}^{n-}\cdot mH_2O$, where M^{2+} and M^{3+} are divalent and trivalent cations that occupy octahedral positions in the hydroxide layers, A^{n-} is an interlayer anion and x is defined as the $M^{3+}/(M^{2+} + M^{3+})$ ratio. Their basic property and interlayer anion exchangeability make them potent catalysts, as well as adsorbents, anion exchangers, acid residue scavengers, stabilizers for polymer etc. [1–4].

LDHs are potential materials for flame retardants, due to the high water content in their brucite-like layers and the flame inert anions in the interlayer galleries. However, just like the other solid materials, the compatibility problem between the hydrophilic LDHs and the hydrophobic polymer will be encountered when LDHs are dispersed into polymer matrix. One of the resolutions is to modify the LDH surfaces with organic surfactants or/and coupling agents to change the hydrophilic surfaces of LDHs to hydrophobic ones. Silylation is the most common process especially when organosilanes are with nucleophilic groups (e.g. 3-aminopropyltriethoxysilane, APS) [5–9]. In this case, organosilane can not only increase the hydrophobicity of substrates by the surface grafting, but also help to bond with the polymers by amino groups. Therefore, this method has been extensively applied in the modification of semiconductors, metals, glass, ceramics, and clays etc. [5–9]. Increasing interests were paid to silylation of clays to design nanocomposites in the last

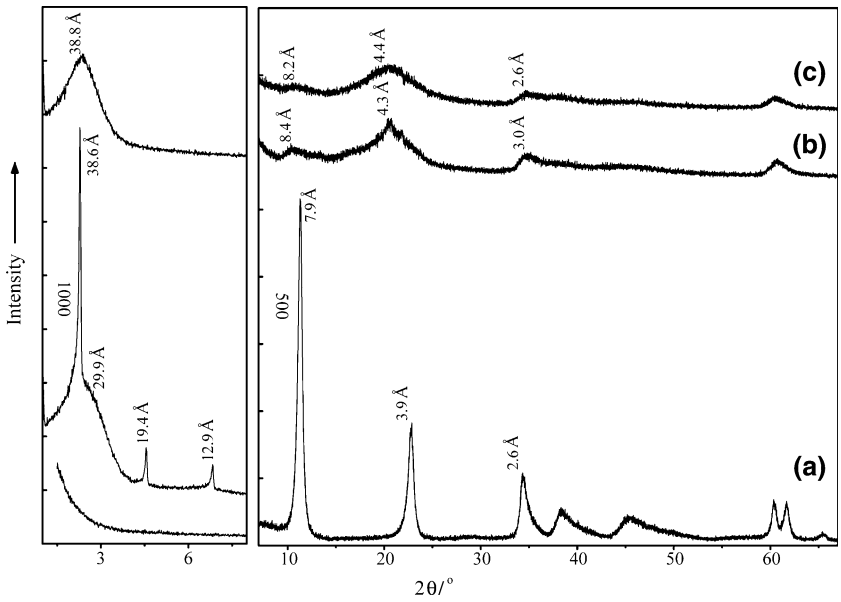

Fig. 1 The XRD patterns of silylated LDH. (a) LDH, (b) H-DS, and (c) H–Si

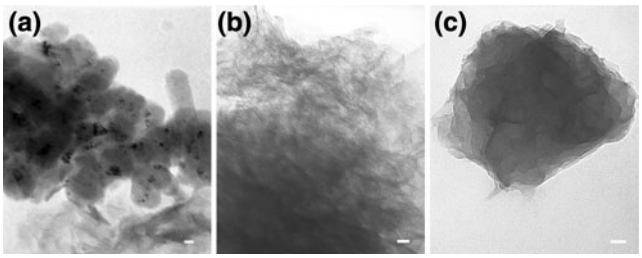

Fig. 2 The TEM images of LDH and silylated LDH. Scale bars are 20 nm

decades. However, most of these researches focused on cationic clay minerals, for example, smectite group minerals and minerals from the serpentine group [10–12]. Very few studies were conducted on the grafting silane onto the surface of LDHs, the only anionic clay existence in nature [13, 14]. The most important reason rests on their higher surface charge density (about one positive charge per 25 $Å^2$ for the case of $x = 0.32$) [15] compared with other clays (e.g., the unit cell charge of smectite clays varied from −0.6 to −1.4 per O_{20} unit) [16]. Such a problem can be overcome using long alkyl chain anions to enlarge the interlayer distance of LDHs. The large organic guest anions can introduce the solvents or non-polar reactants into the LDHs interlayer and to reduce the interaction between the adjacent layers. As a result, the exfoliated single layers suspensions are derived from the organo-LDHs. This methodology provides a new mechanism for the grafting of LDHs with functional groups.

A lot of studies focusing on the thermal properties of various LDHs have been reported [17–20], not only because their structures and compositions can be readily deduced from the thermal analysis (e.g. thermogravimetry, TG), but also considered they usually need activation in certain temperatures when used as catalysts [21, 22]. During these procedures, in order to avoid LDHs from the adsorption of unexpected materials, rehydration after heating treatment and even phase transformation of samples when exposure to the air, in situ technologies were developed for a better understanding of their evolution procedures in the latest decade, such as in situ energy-dispersive X-ray diffraction (EDXRD) [23, 24], Fourier transform infrared emission spectroscopy (FTIR ES, or IES) [25, 26], in situ diffuse reflectance infrared Fourier transform spectroscopy (DRIFTS) [27] etc.

Herein, we report a one-step method to synthesize silylated LDHs with the help of surfactants (sodium dodecylsulfate, SDS). The structure and properties of as-synthesized materials were characterized by X-ray diffraction (XRD) and transmission electron microscopy (TEM). The thermal transformation of anionic surfactant modified and silylated products were investigated by IES and TG measurements. The influences from SDS and APS on the resultant materials were discussed on the basis of their geometrical arrangements, morphology, spectral characteristics, and thermal properties.

Experimental

Synthesis of materials

The hydrotalcites, $Mg_6Al_2(OH)_{16}CO_3{\cdot}4H_2O$, was synthesized by in situ coprecipitation as described previously [28]. Briefly, a mixture of 9.6 g $Mg(NO_3)_2{\cdot}6H_2O$ and 4.7 g of $Al(NO_3)_3{\cdot}9H_2O$ with a molar ratio of 3:1 (Mg^{2+}/Al^{3+}) were dissolved in 44 cm^3 distilled water (Solution A). About 4 g NaOH was dissolved in 50 cm^3 distilled water (Solution B). At room temperature, Solution A was

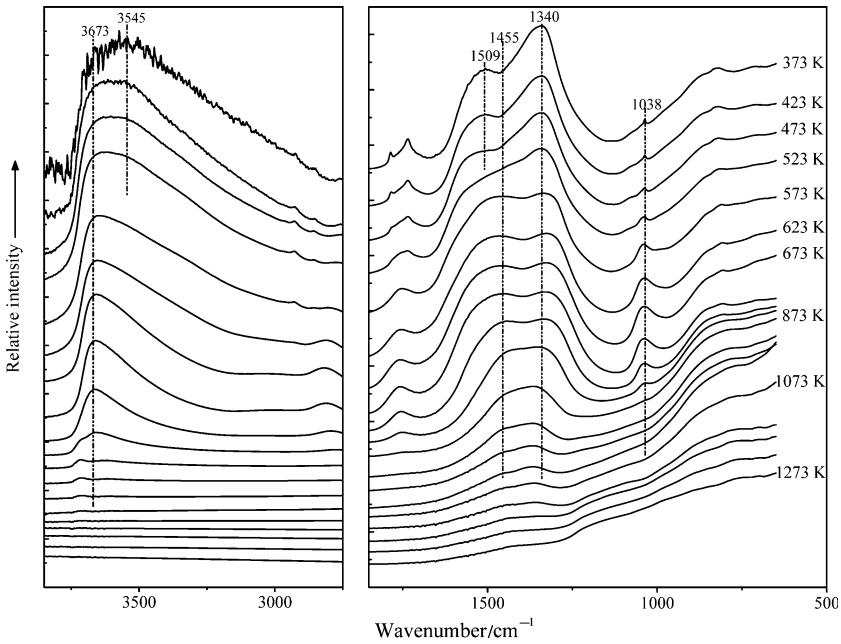

Fig. 3 IES spectroscopy of LDH

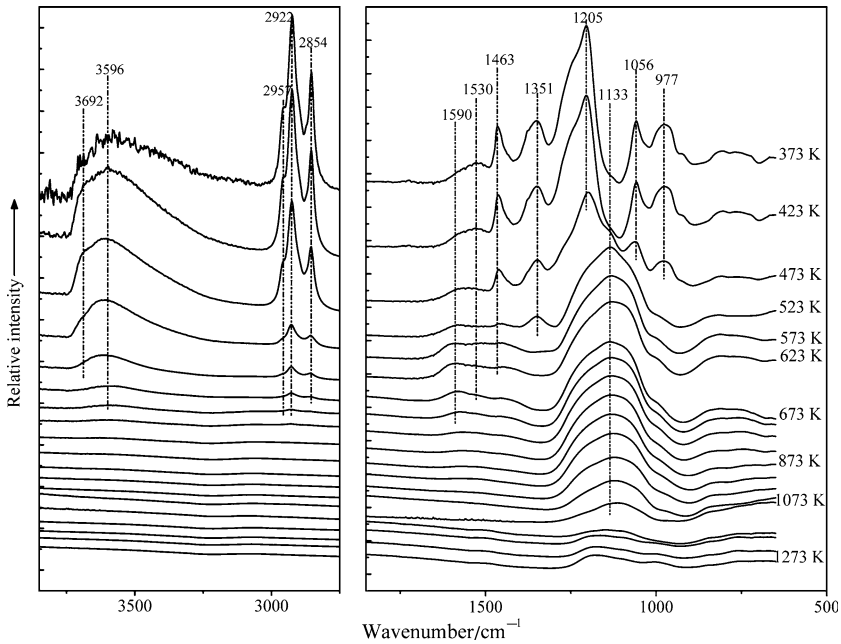

Fig. 4 IES spectroscopy of H-DS

dropped into 50 cm^3 distilled water with vigorous stirring and the mixture was adjusted at around pH = 10 with solution B. After aged at 353 K for 12 h, the obtained slurry was washed with distilled water, and dried at 353 K. The obtained material was denoted as LDH.

The silylated LDH was synthesized as follows. 19.2 g of $Mg(NO_3)_2{\cdot}6H_2O$ and 9.4 g of $Al(NO_3)_3{\cdot}9H_2O$ were dissolved in 90 cm^3 of distilled water (Solution C). Approximately 8 g NaOH and 8.6 g SDS were dissolved in 50 cm^3 distilled water (Solution D). 14 cm^3 APS was dispersed in 50 cm^3 ethanol (Solution E). At room temperature, Solutions C, D, and E were added into 100 cm^3 distilled water. With the same procedure as in LDH synthesis, the silylated LDH was obtained and denoted as H–Si.

Similarly, the only anionic surfactant (SDS) modified LDH was synthesized following the procedure as for H–Si, except for the absence of APS. The obtained material was denoted as H-DS.

Characterization

Powder XRD patterns were recorded using a Bruker D8 Advance diffractometer with Cu K_α radiation ($\lambda = 1.5406°$), operating at 40 kV and 40 mA. The incident beam was

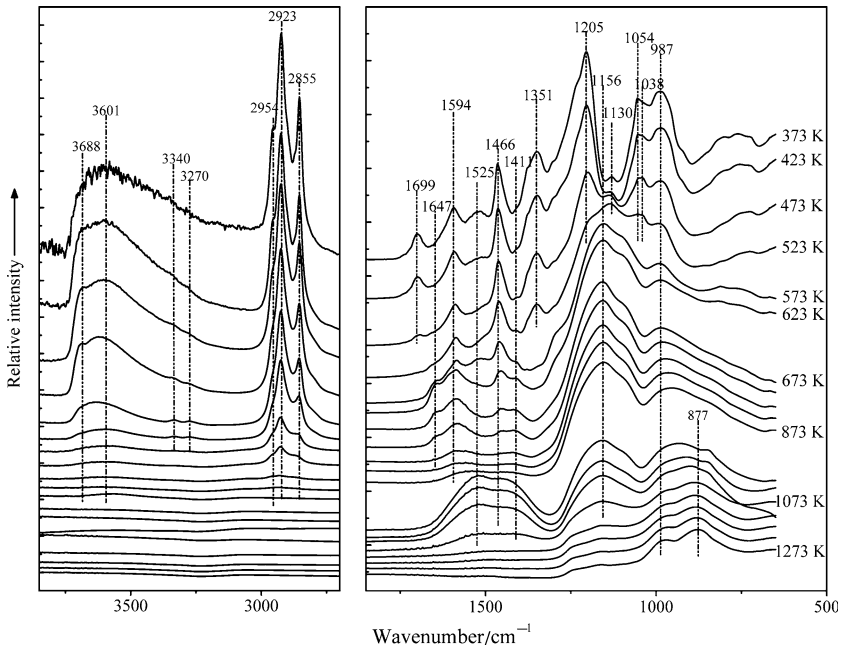

Fig. 5 IES spectroscopy of H–Si

monochromated through a 0.020 mm Ni filter then passed through a 0.04 rad Soller slit, a 1.0 mm fixed mask with 1.0° divergence slit, 0.2° anti-scatter slit, between 1° and 76° (2θ) at a scan speed of 1.5° min^{-1} with an increment of 0.01°.

Infrared emission spectroscopy (IES) was carried out on a Nicolet spectrometer, which was modified by replacing the IR source with an emission cell. Approximately 0.2 mg samples were spread as thin layers on an about 6 mm diameter platinum surface in an N_2 atmosphere. The emission spectra were collected at intervals of 50 K over the range 373–1273 K. Considering both precision and time efficiency, the spectra were acquired by co-addition of 1024 scans for the temperature from 373 to 523 K (about 10 min 34 s each time), 128 scans for the temperature from 573 to 773 K (about 1 min 19 s) and 64 scans for the temperature from 823 to 1273 K (about 40 s), with a resolution of 4 cm^{-1}.

Thermogravimetry (TG) of samples were recorded on a SDT Q600 thermobalance (TA, USA) between 298 and 1273 K with a heating rate of 5 K min^{-1} under N_2 atmosphere (100 cm^3 min^{-1}).

Results and discussions

The X-ray diffraction patterns of synthesized LDH, H-DS, and H–Si are shown in Fig. 1. The XRD pattern of LDH displays a typical and well ordered layer structure with a basal spacing (d_{003}) of 7.9 Å (Fig. 1a). This value well matches with reference pattern 01-070-2150 (pyroaurite—$Fe_2Mg_6(OH)_{16}CO_3(H_2O)_{4.5}$). The morphology of LDH can also be evidenced by TEM image which displays uniform crystal particles (Fig. 2a).

The influence of DS^- intercalation is clearly indicated by the new diffraction sequences in 2 theta angles locating at 2.3°, 4.6° and 6.9°, corresponding to d_{001}, d_{002}, and d_{003}, respectively [29]. Meanwhile the reflections corresponding to residual LDH (10–76°) turn to broadened humps with low intensity (Fig. 1b). The TEM image of H-DS displays fibrous exfoliated layers (Fig. 2b), resulting from the intercalation of surfactants. This is of high importance for uniform distribution of LDH in polymer matrix.

The stacking mode and morphology of H–Si are very different from both LDH and H-DS as shown by both XRD patterns (Fig. 1c) and TEM image (Fig. 2c). Only one broad reflection can be observed in the XRD pattern of H–Si in the range of 1–10° with a d value of 38.8 Å, indicating disturbed anions distribution in the interlayer galleries. The possible explanation is that the H-DS turns to hydrophobic and introduce APS enter the interlayer, which influence the regular arrangement of DS^-. Such a hypothesis was proved by $-CH_2$ vibration and d value changes as discussed in the literature [28]. The TEM image displays large particles with thin curved sheets and rough surfaces, which may result from the silane condensate with the –OH on the LDH surface.

The thermogravimetry and infrared emission spectroscopy of the three samples are shown in Figs. 3, 4, 5, and 6. The TG curve of LDH shows three mass loss stages as dehydration (304–486 K), dehydroxylation (486–673 K), and decarbonation (673–923 K) steps (Fig. 6a). In dehydration stage, three mass loss steps are observed in the DTG curve, corresponding to the loss of extra-surface absorbed water, water in the interlayer galleries and CO_3^{2-} electrostatically attracted on the surfaces, respectively [27].

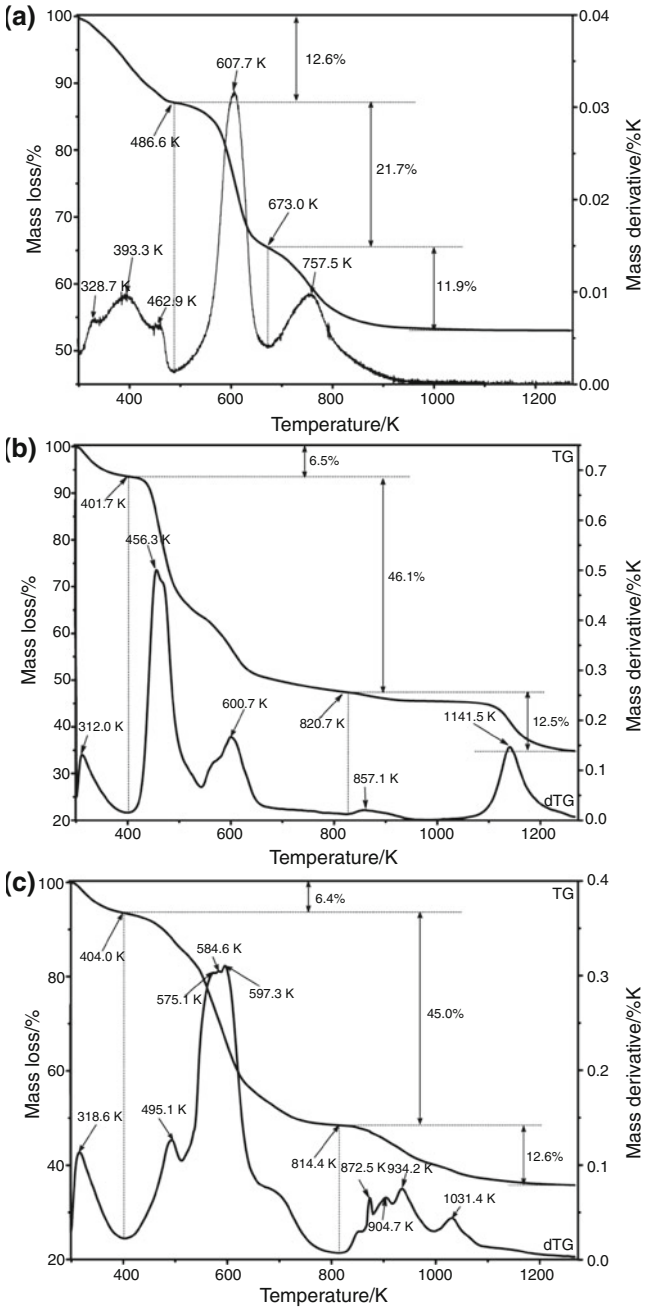

Fig. 6 The TG–DTG curves of LDH (**a**), H-DS (**b**), and H–Si (**c**)

The related IES spectra indicate that the vibration intensity of water gradually decreased and/or disappeared, such as 3350–3050 cm^{-1} corresponding to H-bonds between hydroxyl (–OH) and H_2O and the bridge bond between H_2O and CO_3^{2-}, and around 1510 cm^{-1} due to H_2O bending modes. Dehydroxylation stage begins at ca. 486 K and ends at ca. 673 K with a prominent peak as shown in DTG curve. During this procedure, most hydroxyls of LDH's plates are removed judged from IES spectra (Fig. 3, 473–673 K) with a marked intensity decrease in the region of 3680–3500 cm^{-1}, attributed to M–OH (M = Mg, Al) stretching vibrations. Besides, an evidence of phase transformation to form $MgAl_2O_4$ is also noticed at 1038 cm^{-1}, of which the intensity is increased and peak width is broadened [30]. The intensity of the peak at around 1340 cm^{-1} is also decreased together with a frequency shift at 1510–1480 cm^{-1}, corresponding to the loss of CO_3^{2-}. Starting from 673 K, the interlayered CO_3^{2-} are volatilized, together with further decomposition of $MgAl_2O_4$ to form MgO and Al_2O_3 [29]. The two evolutions finish at about 973 K as shown in Figs. 3 and 6a.

With the intercalation of anionic surfactant, apparent changes are recorded in both IES spectra (Fig. 4) and TG curve (Fig. 6b). First, a significant mass loss due to alkyl chain combustion and dehydroxylation beginning at around 403 K is shown in DTG curve. Accordingly, C–H and –OH related bands gradually disappear in IES spectra, including the vibrations in the region of 3750–3300 cm^{-1} for –OH stretching modes, in 2960–2850 cm^{-1} for C–H stretching modes and at around 1350 cm^{-1} for $–CH_2–$ wagging modes. Second, a series of bands corresponding to $–OSO_3^-$ are observed at 1205, 1056, and 977 cm^{-1}. Most of these bands decrease in intensity obviously at around 523 K, but the weak vibrations can be seen even up to 1073 K. Third, the –OH related bands shift to higher wavenumbers, and the bands due to H-bond between H_2O and anions and/or –OH are reduced as shown in the region of 3750–3000 cm^{-1} of IES spectroscopy and 373–413 K of TG–DTG curves. Besides, a board peak centered at around 1133 cm^{-1} is displayed from 473 to 1273 K (Fig. 4), attributed to $NaHSO_4$ formed and evolved during heating [29], correspondingly, a mass loss procedure is noticed begin from 823 K.

Grafting APS onto the surface of LDH results in the occurrence of a group of new bands at 3270 ($–NH_2$ stretching), 1590 ($–NH_2$ scissoring), 1038 (Si–O–C asymmetric stretching) and 987 cm^{-1} (Si–O–M stretching) as observed in the IES spectra of H–Si (Fig. 5, 373 K). Accordingly, the APS related thermal decomposition can be observed from both TG curve and IES spectra of H–Si (Figs. 5, 6c). Similar to that of H-DS, the decrease of interlayer water content is shown from the TG curve of H–Si. The three weak peaks indicated in dehydration stage of LDH now become only one, and the water content decreased to 6.4%. This decrease may due to the increase of surface hydrophobicity of surfactant modified samples along with the water consumption of APS further hydrolysis to form Si–OH in the interlayer space of LDH. The alkyl chain combustion and dehydroxylation process are split into two stages centered ca. 495 and 575 K, respectively. However, these two procedures overlap each other as judged from the –OH and C–H bands changes tendency in IES spectra (423–573 K). During this process, the intensity of Si–O–M relevant band gets slightly weak

(987 cm^{-1}), while that of Si–O–C related band maintains (1038 cm^{-1}). The $–OSO_3^-$ stretching modes (1056 and 977 cm^{-1}) are still distinguishable up to 523 K. With the temperature rising from 573 to 823 K, another quick mass loss procedure is noticed in TG curve. During this procedure, all the signals in IES spectra above 1300 cm^{-1} are faded away gradually, corresponding to the further loss of –OH (3700–3300 cm^{-1}), C–H (3000–2800, 1466 cm^{-1}) and $–NH_2$ (1594, 1925 cm^{-1}) etc., while the bands attributed to Si–O stretching (987 cm^{-1}) and $–OSO_3^-$ stretching modes remain (1054 cm^{-1}). Furthermore, a new broad band centered at 1156 cm^{-1} is generated and its intensity maintains during this heating process. This band also exist in the IES of H-DS at around 1133 cm^{-1} in the same temperature region, therefore it is again assigned to the formation of $NaHSO_4$. The final step involves $NaHSO_4$ decomposition and decomposition of $MgAl_2O_4$ to form Na_2O, SO_3, MgO, Al_2O_3 and H_2O [29] etc. Compared with that of H-DS, two extra broad peaks in region of 1650–1300 cm^{-1} and region of 900–800 cm^{-1} are observed in the IES spectra of H–Si attributed to overtone of Si–O and Si–O–Si symmetric stretching modes, respectively.

Conclusions

By an in situ coprecipitation method, the anionic surfactant and silane modified layered double hydroxides were synthesized. The silane molecules were introduced to condense with the surface –OH of LDH's by surfactant anions and disturbed the distribution of surfactant anion within interlayer space. The fibrous exfoliated layers in surfactant intercalated LDH changes to curved sheets with rough surface in silylated sample. The thermal decomposition of synthesized samples were studied by infrared emission spectroscopy (IES) combined with thermogravimetry (TG). The alkyl chain combustion and dehydroxylation procedures are overlapped with one another during heating from 373 to 723 K in H-DS and to 873 K in H–Si. Sulfate anion transformation process occurs at 473 K in H-DS and 523 K in H–Si. The derivant of sulfate can exist even up to 1273 K. After further decomposition, the metal oxides and Si–O compounds are formed beginning at around 923 K in silane modified sample.

Acknowledgements This is contribution No. IS-1122 from GIGCAS. The financial and infra-structure supports of the National Science Fund for Distinguished Young Scholars (Grant No. 40725006) and Knowledge Innovation Program of the Chinese Academy of Sciences (Grant No. KZCX2-yw-112) are acknowledged. The financial and infra-structure support of the Queensland University of Technology Inorganic Materials Research Program of the School of Physical and Chemical Sciences is gratefully acknowledged. The Australian Research Council (ARC) is thanked for funding. Qi Tao is grateful to The China Scholarship Council for the overseas funding to visit QUT.

References

1. Seftel EM, Popovici E, Mertens M, Witte K, Tendeloo G, Cool P, et al. Zn-Al layered double hydroxides: Synthesis, characterization and photocatalytic application. Microporous Mesoporous Mater. 2008;113:296–304.
2. Goh KH, Lim TT, Dong Z. Application of layered double hydroxides for removal of oxyanions: a review. Water Res. 2008; 42:1343–68.
3. Othman MR, Helwani Z, Fernando WJN. Synthetic hydrotalcites from different routes and their application as catalysts and gas adsorbents: a review. Appl Organomet Chem. 2009;23:335–46.
4. Fedorov AA, Checkryshkin YS, Rudometova OV, Vnutskikh ZA. Application of inorganic compounds at the thermal processing of polyvinylchloride. Russ J Appl Chem. 2008;81:1673–85.
5. Angloher S, Kecht J, Bein T. Metal-organic modification of periodic mesoporous silica: multiply bonded systems. Chem Mater. 2007;19:5797–802.
6. Ingall MDK, Honeyman CH, Mercure JV, Bianconi PA, Kunz RR. Surface functionalization and imaging using monolayers and surface-grafted polymer layers. J Am Chem Soc. 1999;121:3607–13.
7. Lee H, Dellatore SM, Miller WM, Messersmith PB. Mussel-inspired surface chemistry for multifunctional coatings. Science. 2007;318:426–30.
8. Oh S, Kang T, Kim H, Moon J, Hong S, Yi J. Preparation of novel ceramic membranes modified by mesoporous silica with 3-aminopropyltriethoxysilane (APTES) and its application to Cu^{2+} separation in the aqueous phase. J Membr Sci. 2007;301:118–25.
9. Yeon YR, Park YJ, Lee JS, Park JW, Kang SG, Jun CH. $Sc(OTf)_3$-mediated silylation of hydroxy functional groups on a solid surface: a catalytic grafting method operating at room temperature. Angew Chem Int Ed. 2008;47:109–12.
10. Frost RL, Mendelovici E. Modification of fibrous silicates surfaces with organic derivatives: an infrared spectroscopic study. J Colloid Interface Sci. 2006;294:47–52.
11. Mendelovici E, Frost RL. Pioneer studies on HC1 and silylation treatments of chrysotile. J Colloid Interface Sci. 2005;289:597–9.
12. Mendelovici E, Frost RL, Kloprogge JT. Modification of chrysotile surface by organosilanes: an IR-photoacoustic spectroscopy study. J Colloid Interface Sci. 2001;238:273–8.
13. Park AY, Kwon H, Woo AJ, Kim SJ. Layered double hydroxide surface modified with (3-aminopropyl)triethoxysilane by covalent bonding. Adv Mater. 2005;17:106–9.
14. Wypych F, Bail A, Halma M, Nakagaki S. Immobilization of iron(III) porphyrins on exfoliated MgAl layered double hydroxide, grafted with (3-aminopropyl)triethoxysilane. J Catal. 2005; 234:431–7.
15. Li C, Wang G, Evans DG, Duan X. Incorporation of rare-earth ions in Mg-Al layered double hydroxides: intercalation with an $[Eu(EDTA)]^-$ chelate. J Solid State Chem. 2004;177:4569–75.
16. Kickelbick G. Hybrid materials: synthesis, characterization, and applications. 1st ed. New York: Wiley-VCH; 2007.
17. Voyer N, Soisnard A, Palmer SJ, Martens WN, Frost RL. Thermal decomposition of the layered double hydroxides of formula $Cu_6Al_2(OH)_{16}CO_3$ and $Zn_6Al_2(OH)_1)CO_3$. J Therm Anal Calorim. 2009;96:481–5.
18. Frunza M, Lisa G, Popa MI, Miron ND, Nistor DI. Thermogravimetric analysis of layered double hydroxides with chloramphenicol and salicylate in the interlayer space. J Therm Anal Calorim. 2008;93:373–9.

19. Palmer SJ, Spratt HJ, Frost RL. Thermal decomposition of hydrotalcites with variable cationic ratios. J Therm Anal Calorim. 2009;95:123–9.
20. Stanimirova T, Balek V. Characterization of layered double hydroxide Mg-Al-CO_3 prepared by re-hydration of Mg-Al mixed oxide. J Therm Anal Calorim. 2008;94:477–81.
21. Reichle WT. Catalytic reactions by thermally activated, synthetic, anionic clay minerals. J Catal. 1985;94:547–57.
22. Pesic L, Salipurovic S, Markovic V, Vucelic D, Kagunya W, Jones W. Thermal characteristics of a synthetic hydrotalcite-like material. J Mater Chem. 1992;2:1069–73.
23. Williams GR, Norquist AJ, O'Hare D. Time-resolved, in situ X-ray diffraction studies of staging during phosphonic acid intercalation into [LiAl2OH$_6$]Cl·H_2O. Chem Mater. 2004;16:975–81.
24. Williams GR, Dunbar TG, Beer AJ, Fogg AM, O'Hare D. Intercalation chemistry of the novel layered double hydroxides [$MAl_4(OH)_{12}$](NO_3)$_2$·γH2O (M = Zn, Cu, Ni and Co). 1: new organic intercalates and reaction mechanisms. J Mater Chem. 2006;16:1222–30.
25. Kloprogge JT, Frost RL. Infrared emission spectroscopic study of the thermal transformation of Mg-, Ni- and Co-hydrotalcite catalysts. Appl Catal A-Gen. 1999;184:61–71.
26. Kloprogge JT, Frost RL. Infrared emission spectroscopy of clay minerals. In: Kloprogge JT, editor. Application of vibrational spectroscopy to clay minerals and layered double hydroxides. Aurora: The Clay Minerals Society; 2005. p. 99–124.
27. Yang WS, Kim Y, Liu PKT, Sahimi M, Tsotsis TT. A study by in situ techniques of the thermal evolution of the structure of a Mg–Al–CO_3 layered double hydroxide. Chem Eng Sci. 2002;57:2945–53.
28. Tao Q, He HP, Frost RL, Yuan P, Zhu JX. Nanomaterials based upon silylated layered double hydroxides. Appl Surf Sci. 2009;255:4334–40.
29. Clearfield A, Kieke M, Kwan J, Colon JL, Wang RC. Intercalation of dodecyl sulfate into layered double hydroxides. J Inclusion Phenom Macrocycl. 1991;11:361–78.
30. Gadsden JA. Infrared spectra of minerals and related inorganic compounds. London: Butterworths; 1975.